Guest Binding and Orientation within Open Nanoscale Hosts

Zachary R. Laughrey, Corinne L. D. Gibb, Tangi Senechal, and Bruce C. Gibb*[a]

Abstract: The synthesis of three different nanoscale molecular hosts is reported. These cavitands each possess a highly preorganized cavity with an open portal (nearly 1 nm wide), by which guests can enter and egress the cavity. Additionally, these hosts are deep-functionalized with a crown of weakly acidic benzal C–H groups which can form a variety of noncovalent interactions with guest molecules residing within the cavity. Thirty-one guests were examined for their propensity to form complexes with the hosts. Guests that possess halogen atoms were the strongest binders, suggesting the formation of polydentate C–H···X–R hydrogen bonds with the deep crown of benzal hydrogens. Exchange rates between the free and bound states were noted to be dependent on the size of the guest and the solvent used to study complexation. In general, stronger binding and slower exchange were noted for complexations carried out in DMSO with highly complementary guests. The orientation of each guest within the cavity was determined using either EXSY NMR spectroscopy or ^{1}H NMR shift data. Cumulatively these results showed that the principal factors directing orientation were interactions with the benzal groups and the type of solvent. Van't Hoff analyses of selected complexations were also carried out. As well as revealing that all complexations were entropically unfavorable, these experiments provided support for guest orientation determinations, and gave an estimation that the formation of a C–H···I–R hydrogen bond releases between 1 and 1.5 kcal mol^{-1}.

Keywords: cavitands · host–guest systems · nanostructures

Introduction

The precise orchestration of noncovalent and covalent forces lies at the heart of enzyme catalysis. One way to begin to understand this orchestration is enzyme mimicry; the replication[1] of the active site of the target enzyme using a small molecule. One facet of an enzyme that is difficult to replicate is the hydrophobicity of the active site. Active-site walls must be constructed. One approach is to construct the concave molecular surface by designing a polymer that will fold into a predesigned topology.[2, 3] Another is to borrow from Nature and try and decorate the inner surfaces of a cavity in, for example, cyclodextrins.[1e] Alternatively, the task can be approached by building a suitably functionalized molecular cavity "brick-by-brick". Building up a host with a large hydrophobic cavity is complicated by the possibility of molecular collapse. Thus although relatively small rigid cavities have been built using calixarenes,[4] resorcinarenes,[5] and cyclotriveratrylenes,[6] there have been relatively few reports concerning the synthesis of hosts with nanoscale cavities.[7, 8] Furthermore, although introducing functionality into small or flexible cavities has been considered for some time,[9] adding functionality to large, organized cavities is only just beginning to be addressed.[10]

We describe here the synthesis of nanoscale hosts, the molecular surfaces of which are woven using only covalent bonds. This feature helps to endow these molecules with highly preorganized cavities. Their general design includes an open portal for guest entry and deep functionalization in the form of a "crown" of slightly acidic benzal hydrogens situated 6 Å down into the binding pocket. This array is capable of forming (up to) five centered, or tetrafurcated acceptor type, hydrogen bonds with guests possessing halogen atoms. Consequently, along with the nature of the solvent, this array is an important contributor to both guest selection and orientation.

Results and Discussion

Host synthesis: The synthesis of molecular baskets **3**–**5** (Scheme 1) utilizes the stereoselective bridging of resorcinar-

[a] Prof. B. C. Gibb, Z. R. Laughrey, C. L. D. Gibb, T. Senechal
Department of Chemistry, University of New Orleans
New Orleans LA 70148 (USA)
Fax: (+1) 504-280-6860
E-mail: bgibb@uno.edu

Supporting information contains ^{1}H NMR, COSY NMR, and NOESY NMR spectra of the three hosts, EXSY NMR spectra of selected complexes, a summary of binding protocols, tables of complex-induced NMR shift data for host **3** binding guests **G1**–**G31** in $CHCl_3$, [D_8]toluene, and [D_6]DMSO, and a brief summary of computational approaches to conformational flipping in host **4**. Supporting information for this article is available on the WWW under http://www.chemeurj.org/ or from the author.

0947-6539/03/0901-0130 $ 20.00+.50/0 *Chem. Eur. J.* **2003**, *9*, No. 1

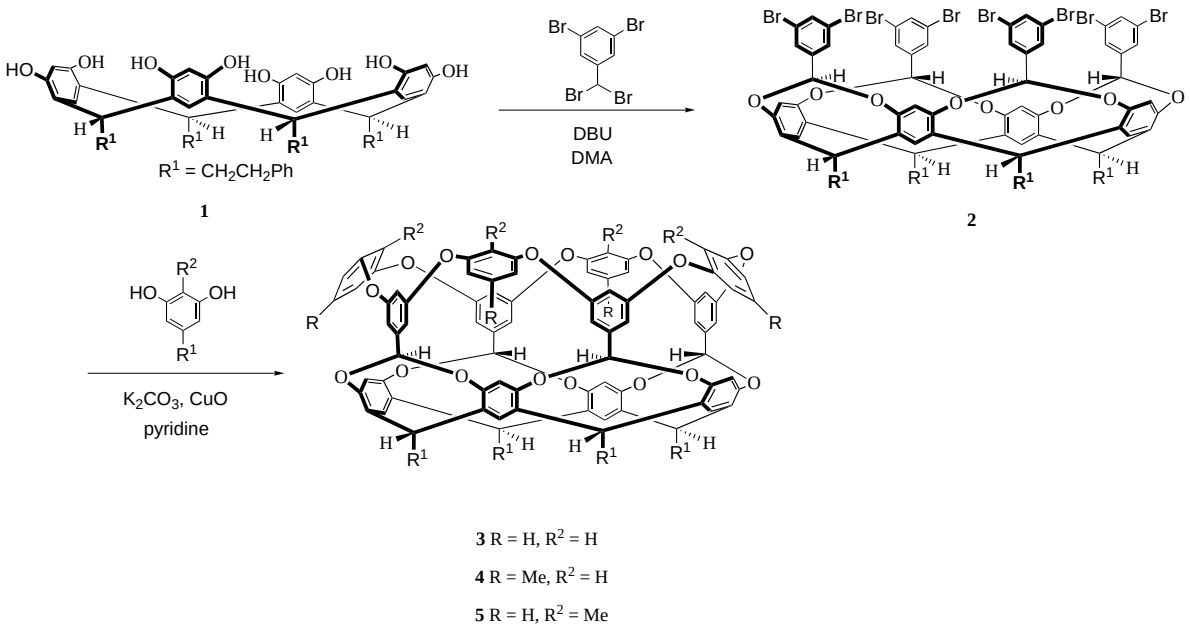

Scheme 1. The synthesis of molecular baskets **3**–**5**.

enes, for example, **1**, with benzal bromides.[11] Thus, bridging the phenolic pairs of **1** with 3,5-dibromobenzal bromide[12] gave key octabromide deep-cavity cavitand (DCC) **2** in 65% yield (Scheme 1).[11b] This introduction of a second row of aromatic rings into the resorcinarene scaffold deepens the cavity of the resorcinarene framework considerably. However, a lack of preorganization of the benzal bridges results in these compounds possessing poor hosting properties. One way to preorganize **2** is to covalently bridge between each of the aromatic rings in the second row. We selected the Ullmann aryl ether reaction for this purpose primarily because the introduction of four resorcinol moieties would afford a high degree of rigidity to the rim of the resulting cavitand. Initial attempts at this eightfold reaction using recently developed catalytic approaches unfortunately proved unsuccessful in our hands.[13] However, using more classical conditions of pyridine as solvent, potassium carbonate as base, and copper(II) oxide as promoter, gave molecular basket **3** in a very satisfying 88% yield.[7a] Each of the eight new C–O bonds are formed in greater than 98.5% efficiency. With this success, we considered other resorcinols that might be amenable to this reaction. We chose 5-methyl resorcinol and 2-methyl resorcinol; the former because the methyl groups could potentially alter the portal size of the resulting basket **4**, and the latter because the resulting basket **5** was anticipated to have different structural dynamics compared with **3** and **4** (vide infra). Gratifyingly, reaction of **2** with 5- and 2-methyl resorcinol gave the respective hosts **4** and **5** in 80% and 88% yields, respectively (Scheme 1). COSY NMR spectroscopy was necessary for the full assignment of the protons in hosts **3**–**5** (see Supporting information).

Host dynamics: Inspection of models indicated that the third row of rings in hosts **3**–**5** have conformational options. Two (extreme) conformations can be envisaged. For example, host **3** can theoretically adopt one conformation with all four rings oriented outwards so as to reveal a deep cavity with a circular 1 nm wide entrance, or the conformation, in which all four rings are oriented inwards (Figure 1). In the latter case

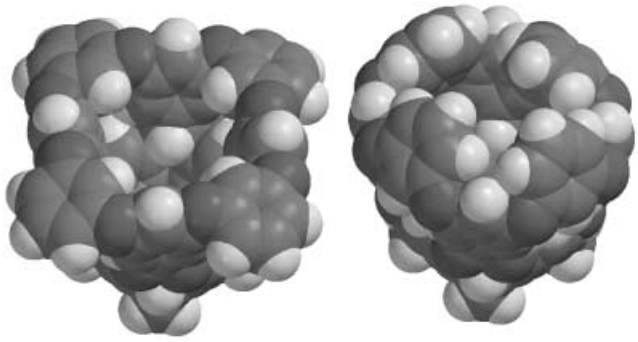

Figure 1. The open and closed conformations of molecular basket **3**.

the entrance to the cavity is much smaller. Host **4** was expected to show similar conformation properties. However, because of the position of the methyl groups, the all-closed conformation would possess only the smallest of apertures. In **5**, the methyl groups were expected to affect the rate of interconversion between the conformers since during this process they must pass through a relatively small annulus (above H_e in Scheme 2). Furthermore, the open conformer of **5** (methyl groups in) would have a much smaller cavity.

A combination of 2D NOESY NMR for **3** and **5**, and 1D NOE for **4** (solutions of which precipitated over the time frame of a 2D experiment) revealed the conformational preferences of these hosts in [D_6]DMSO. In each case, a strong NOE was observed between protons H_f and H_g (Scheme 2) which suggested an open conformation. In contrast there were no cross peaks corresponding to an H_d and H_g interaction as would be expected in the closed conformation. Computational work (gas phase) offers support for these

  0947-6539/03/0901-0131 $ 20.00+.50/0

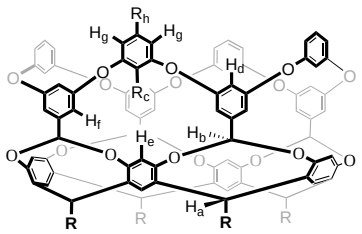

Scheme 2. "Proton" designation in the molecular baskets: **3** (R_c and R_h = H), **4** (R_c = H, R_h = Me), and **5** (R_c = Me, R_h = H).

findings. Thus, semiempirical calculations (modified neglect of diatomic overlap (MNDO)) on both the open and the closed conformations of each basket[14] were in line with similar calculations we had performed earlier on **3**.[7c] The heats of formation for the open conformation of **3**, **4**, and **5** were calculated to be 9, 9, and 17 kcal mol^{-1}, respectively, lower in energy than their corresponding closed conformation. These hosts are anancomeric.

How large are the energy barriers between these conformations? Solutions of the hosts in CD_2Cl_2 were examined down to $-90\,^{\circ}C$ for evidence of the decoalescence that would occur as the conformational flipping slowed to a timescale less than the NMR timescale. No broadening of signals was apparent for those protons most likely to be affected by conformational "freezing", that is, H_c, H_f, H_g, and H_h (or the corresponding methyl groups).[15] This result can be explained either in terms of the anancomeric nature of the hosts, or that the energy barrier to flipping *each* aromatic ring is less than 9 kcal mol^{-1}.[16] Indeed, calculations suggest both these points are valid for **3** and **4**. Thus, for these hosts, the energy barriers between the conformer with all four rings in a closed conformation and the conformation, in which *one* ring adopts an open position, were both calculated to be 6.5 kcal mol^{-1} (Supporting information). Although a value of 18 kcal mol^{-1} was calculated for **5**, no decoalescence was observed. Presumably, the anancomeric nature of **5** precludes observing decoalescence.

To summarize, these hosts exist primarily in an all-ring open conformation. However, the stepwise flipping of one ring into a closed position is a relatively facile process.

Guest selection and orientation: The cavity volumes of **3** and **4** are estimated to be in the region of 280 Å^3, while with four methyl groups pointing into the cavity, the volume of **5** is estimated to be about 200 Å^3. As discussed, these hosts have fully open and solvated cavities. Hence, it can be expected that guest binding will be dependent on the solvent.[17] Inspection of models suggests that quasispherical adamantanes are ideal guests for **3** and **4**. Host **5** on the other hand possesses a cavity that is too small for adamantanes. To build a binding profile for these two cavity shapes we chose a list of guests from bromocyclobutane, up to bromocamphor (Scheme 3). Guest binding induces shifts in several NMR signals from the host and all of those from the guest. However, unless noted, we chose the benzal protons H_b to measure association constants because they underwent large shifts and, barring the signal from H_a, are well removed from other signals (Figure 2).

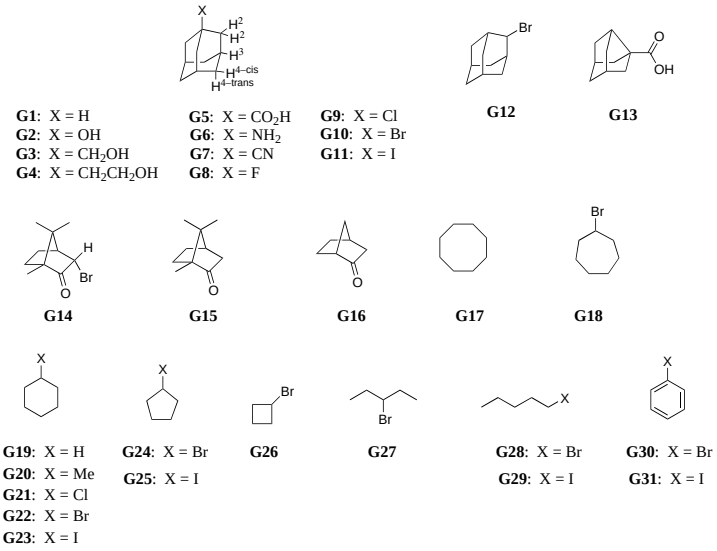

Scheme 3. Guests used in this study.

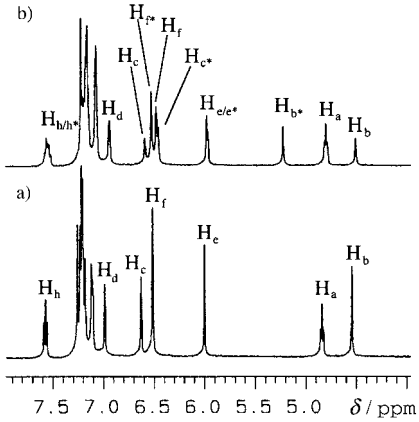

Figure 2. a) Selected region of the ^{1}H NMR spectrum of host **3** in $CDCl_3$; b) Host **3** complexed with guest **G11** in $CDCl_3$. Exchange is slow on the NMR timescale and allows identification of signals from both free and bound (*) protons. Proton designations are shown in Scheme 2.

The C_{4v} symmetry of these hosts means that as well as the strength of association, we also have to be mindful of guest orientation. In this regard, 2D EXSY ^{1}H NMR spectroscopy proved useful[18] for those systems, in which exchange was slow on the NMR timescale. Figure 3 shows part of the 2D EXSY spectrum of the complex **G14@3** in [D_6]DMSO, the observed signal shifts, and a picture derived from a molecular mechanics calculation of the complex. As is seen with smaller cavitands, the conical profile to the cavity results in the

  0947-6539/03/0901-0132 $ 20.00+.50/0 *Chem. Eur. J.* **2003**, *9*, No. 1

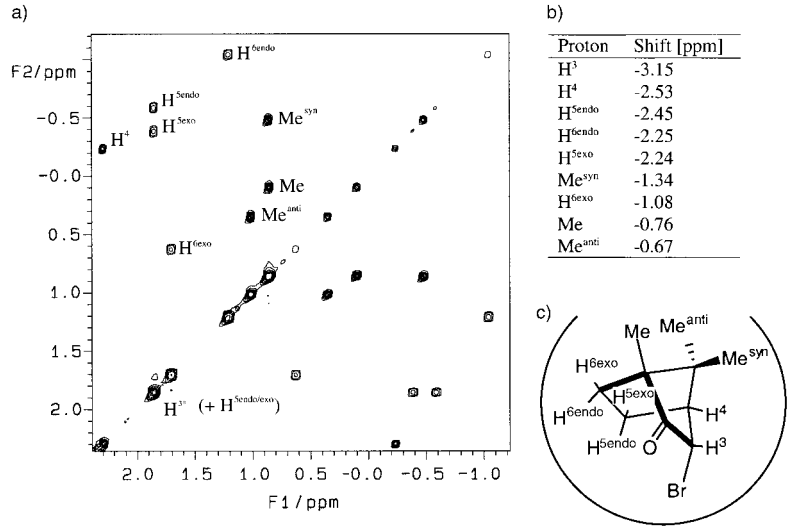

Proton	Shift [ppm]
H^3	-3.15
H^4	-2.53
H^{5endo}	-2.45
H^{6endo}	-2.25
H^{5exo}	-2.24
Me^{syn}	-1.34
H^{6exo}	-1.08
Me	-0.76
Me^{anti}	-0.67

Figure 3. a) Part of the 2D EXSY NMR spectrum of **G14** complexed to basket **3**. Cross peaks for protons in the free and bound state are labeled (see structure). Only the signal for proton H^3 in the bound state (H^{3*}) is shown; b) The calculated shifts in the guest's signals upon binding; c) a representation of the guest orientation (as determined by molecular mechanics) demonstrating the correlation between the magnitude of shift with the position (depth) of each proton in the hydrophobic pocket.

general trend that the deeper a proton resides, the more that proton is shielded. Consequently the most shielded protons are H^3, H^4, and the *endo* protons at positions 5 and 6, while those least affected reside at the open end of the cavity near the C_4 axis of the host. One particularly striking pair of shifts is seen for the C^6 methylene group. One proton is shifted $\delta =$ 1.08 ppm upfield, while the other is shifted 2.25 ppm. These hosts may make useful NMR shift reagents for bicyclics in general. EXSY NMR spectroscopy was also useful for determining the orientation of those adamantane guests that exchanged slowly on the NMR timescale. Upon binding, the difference between the shifts in the signals from the H^2 (see Scheme 3) and the H^4 protons ($\Delta\Delta\delta_{H2-H4\text{-trans}}$) revealed the propensity to bind in a particular manner. Thus for guests that displayed principally one orientation in the cavity, $\Delta\Delta\delta_{H2-H4\text{-trans}}$ was found to be large ($> \pm 1$ ppm). However if a guest did not demonstrate a preferential orientation, $\Delta\Delta\delta_{H2-H4\text{-trans}}$ tended towards zero (see Supporting information).

Most of the smaller guests underwent exchange faster than the NMR timescale. For these cases we inferred the orientation of the guest by comparing the shift in the signal H_b and relating this to slow exchanging analogues (see Supporting information). Thus by a combination of EXSY and shift NMR data we were able to deduce the principal orientation of all the functionalized guests and monitor how these were adjusted by solvent changes.

Host properties of basket 3: Table 1 lists the association constants of thirty-one guests examined for three different solvents: [D_1]chloroform, [D_8]toluene, and [D_6]dimethyl sulfoxide (DMSO). Some of the data in the first two columns of this table have been reported previously,[19] but we include them here to emphasize the trend that, with only one exception, binding is strongest in DMSO and weakest in chloroform.

Adamantane (**G1**) serves as a reference point for the other guests investigated. Binding is nonexistent in $CDCl_3$, around 1.6 kcal mol^{-1} in "neutral" toluene, and just under 4 kcal mol^{-1} in DMSO.[20] Upon binding, there is an upfield shift in the signal from the H_b protons. We envisage that **G1** is capable of freely tumbling within the confines of **3**. **G1** binds more strongly to **3** than the series of monofunctionalized adamantyl guests **G2**–**G8**. One important reason why this is so is that the entropy of complexation (vide infra) is larger for **G2**–**G8** because these guests must adopt only one of two conformations (functional group "up" or

Table 1. Association constants between basket **3** and a variety of guests at 298 K.[a]

Guest	$CDCl_3$ [M^{-1}]	[D_8]Toluene [M^{-1}]	[D_6]DMSO [M^{-1}]
G1	–	15	790
G2	–	–[b]	180
G3	–	–[b]	310
G4	–	–[b]	280
G5	–	–	320
G6	–	–[b]	520
G7	–	36	160
G8	–	–	400
G9	53	310[c]	3600[d]
G10	290	1600	33 000[e]
G11	670	4400	140 000[e]
G12	78	380[c]	9800
G13	–	–	97
G14	–	150	1010
G15	–	30	280
G16	–	29	5
G17	–	–	76
G18	5	24	330
G19	–	–	13
G20	–	–	33
G21	–	–	43
G22	–	13	180
G23	7	35	580
G24	–	7	76
G25	–	17	200
G26	–	–	9
G27	–	–	45
G28	–	–	–
G29	–	–	9
G30	–	–	7
G31	–	–	15

[a] Error within ± 10% from average of at least three titrations. Except as noted determinations were made directly using H_b or H_c (see Scheme 2). The symbol "–" denotes that binding was not observed. [b] Determination of association constant was not possible (see reference [21]). [c] Determinations were made by subtraction of H_e from $H_a + H_{b^*}$. [d] Calculated using signals from the C^2 and C^3 positions of the guest (see Scheme 3). [e] Calculated by a competition experiment with adamantane (see Supporting information).

  0947-6539/03/0901-0133 $ 20.00+.50/0

"down"). EXSY NMR spectroscopy demonstrated that **G2**–**G5** bind with their functional groups pointing out of the cavity ($\Delta\Delta\delta_{H2-H4\text{-}trans} \approx +1.2$ ppm). As was observed for the binding of **G1**, these guests all cause an upfield shift (ca. 0.2 ppm) in the signal from H_b because the hydrocarbon moiety of these guests is at the base of the cavity. In contrast, guests **G6**–**G8** show a gradual, increasing tendency to bind with the functional group down. The $\Delta\Delta\delta_{H2-H4\text{-}trans}$ values were ≈ 0, -0.2, and -0.7 ppm, respectively. However, a comparison of the $\Delta\Delta\delta_{H2-H4\text{-}trans}$ values in **G8@3** demonstrates that the tendency for **G8** to bind halogen down is relatively small compared with the other haloadamantanes (vide infra).

In toluene, in which the binding of **G2**–**G8** is faster than the (500 MHz) NMR timescale, a number of differences are observed. Although binding constants for **G2** through to **G6** could not be determined,[21] it was still possible to determine their mode of binding by monitoring shifts in the signal from H_b. In this solvent, the signal H_b shifted downfield when guests **G2**–**G7** bound, a result that indicates that these guests bind primarily with the functional group down. To confirm this, complexes **G2@3**, **G3@3**, and **G6@3** were examined by using 1D NOE NMR spectroscopy, under conditions of slow exchange ([D_8]toluene, $-20\,^{\circ}C$). These experiments confirmed the guest orientations. Thus although **G7** binds down in DMSO and toluene, the preferred orientations of **G2**–**G6** can be switched by changing the solvent. Fluoroadamantane (**G8**) stands out from the list **G2**–**G8** because its small functional group results in no preferred orientation.

For the other adamantoid guests **G9**–**G12**, binding is strong, and only the functional group down orientation is observed (e.g., $\Delta\Delta\delta_{H2-H4\text{-}trans}$ for **G11@3** $= -1.95$ ppm). The strength of binding increases as the halogen increases in size and becomes easier to polarize, to the point that binding of **G11** to **3**, in either toluene or DMSO, is 3 kcal mol^{-1} stronger than the corresponding value for **G1**. Although **G11** has a strong dipole moment,[22] this added stability does not appear to be wholly based on dipole–dipole interactions. **G8** has the highest dipole of the guests (3.92 debyes)[22] but is not strongly bound to **3**. The X-ray structure of **G11@3**[7a] is revealing. In the solid state, the iodine atom of the guest is not situated at the very base of the cavity. Instead, it is aligned with the crown of benzal hydrogens such that the guest hovers over a small cavity. Furthermore, the iodine atom is close to being the perfect fit for the crown. The distance between the halogen atom and each hydrogen (3.077 Å) is slightly less than the sum of the van der Waals radii for I and H (3.35 Å). In other words, there are four C–H$\cdots$X–R interactions in the structure. In the broadest terms, a hydrogen bond is said to exist when:[23] 1) there is evidence of a bond; 2) there is evidence this bond sterically involves a hydrogen atom already bonded to another atom. Thus, **G11@3** is stabilized by a five-centered, or tetrafurcated acceptor type, hydrogen bond. The unusual nature of these interactions is worthy of further comment. Hydrogen bonds are made up of a number of individual components, including electrostatics, polarization, exchange repulsion, charge transfer, and dispersion, that collectively form an attractive force.[24] The most familiar hydrogen bonds[25] are predominantly electrostatic in nature. However in weak hydrogen bonds,[26] the electrostatic component is small, and the dispersion term becomes more important. To date, evidence for these types of hydrogen bonds is limited,[27] but the primary cause of their controversial nature is that they have previously only been observed in solid-state structures, in which it is impossible to determine if they are actually attractive. The association constants tabulated here therefore represent the first *quantitative* glimpse of these types of hydrogen bonds. A crude estimate that ignores differences in the entropy change upon binding **G1** and **G11** indicates that in the case of iodonated guests such as **G11** there is a contribution of at least 0.75 kcal mol^{-1} per C–H$\cdots$I–R hydrogen bond.

A consideration of the data provided in Table 1 reveals how quickly the affinity between **3** and the guests drops off as the guest becomes smaller and/or less complementary to the shape of the cavity. For example, removing a methylene group from **G5** (to give **G13**) causes a 0.72 kcal mol^{-1} drop in the free energy of complexation. Some interesting information can also be garnered from the bicycles studied. Bromocamphor derivative **G14** ($C_{10}H_{15}BrO$) binds more weakly to **3** than the similarly sized **G10** ($C_{10}H_{15}Br$), even though both bind in a bromine atom down orientation. Models indicate that the location of the carbonyl group and the overall lower symmetry of **G14** are the principal causes of the weaker binding. Removal of the bromine atom of **G14** means that camphor (**G15**) binds much more weakly. In DMSO, EXSY NMR spectroscopy demonstrates that the bridgehead methyl group resides in the base of the cavity which results in a downfield shift of the signal from H_b. The similar downfield shift in the signal from the benzal protons upon complexing **G15** in toluene suggests a similar mode of binding in this solvent. Without any methyl groups to pack the base of the cavity, the binding of norcamphor (**G16**) is much weaker. Interestingly **G16** is unique among all the guests examined because it binds more strongly in toluene than in DMSO. Precisely why this is so remains unknown.

In chloroform or toluene, the binding of smaller molecules to **3** was so weak that very few of the guests **G14**–**G31** bind. In DMSO however, solvent competition for the cavity dropped off, and binding for molecules as small as **G26** was observed. The guest series **G18**, **G22**, **G24**, and **G26**, in which a methylene group is removed consecutively from each guest, is illustrative of how quickly the association constants decrease. The loss of three methylene groups means that the binding energy of **G26** to **3** is a full 2 kcal mol^{-1} lower than that for **G18**. Finally, the binding of the cyclohexyl derivatives **G19**–**G23** revealed both the expected trend, and that a methyl group results in weaker binding than an isosteric chlorine atom.

Host properties of basket 4: We began with an investigation of the ability of **4** to bind a number of substituted adamantanes (Table 2). The determined association constants in chloroform were very close to those of basket **3**. However, it was evident that binding in toluene and DMSO was stronger. In these solvents, all the recorded association constants were significantly greater than those recorded for **3**, with the K_a for **G9** binding to **4** double that for host **3**. Again, **G11** proved to be the strongest binder (7.3 kcal mol^{-1}). The orientations of

0947-6539/03/0901-0134 $ 20.00+.50/0 *Chem. Eur. J.* **2003**, *9*, No. 1

Table 2. Association constants between basket **4** and a variety of guests at 298 K.[a]

Guest	$CDCl_3$ [M^{-1}]	[D_8]Toluene [M^{-1}]	[D_6]DMSO [M^{-1}]
G1	–	11	1100
G7	–	36	200
G8	–	–	600
G9	56	520[b]	6000[b]
G10	240	2300	45000[c]
G11	740	7000	220000[c]
G12	77	440[b]	17000
G22	–	–	270
G23	–	–	1100
G24	–	–	85
G25	–	–	380
G28	–	–	–
G29	–	–	10
G30	–	–	8
G31	–	–	19

[a] Errors are within ±10% for an average of at least three titrations, with the exception of guest **G11** binding in DMSO (associated error is ±20% for three titrations). Except as noted determinations were made directly using H_b or H_c (see Scheme 2). The symbol "–" denotes that binding was not observed. [b] Determinations were made by subtraction of H_e from $H_a + H_{b*}$. [c] Calculated by a competition experiment with adamantane (see Supporting information).

the guests in host **4** were the same as those observed for basket **3**. Thus irrespective of the solvent, the halogenated guests always oriented with the halogen down. Likewise, the cyano group of **G7** pointed downwards in toluene, but had a much smaller propensity to do so in [D_6]DMSO ($\Delta\Delta\delta_{H2-H4\text{-trans}} \approx -0.351$ ppm). For smaller guests, the general trend observed for complexations to **3** was reproduced, but again association constants were generally larger. Not all these differences were statistically significant; however differences as large as 95% were seen for **G23**, in which binding is 0.4 kcal mol^{-1} stronger than it is to **3**. Apparently, the remote methyl groups are capable of influencing the binding of guests into these cavities.

Host properties of basket 5: The smaller cavity of **5** resulted in it being a poor host for adamantanes (Table 3). For this host,

Table 3. Association constants between basket **5** and a variety of guests at 298 K.[a]

Guest	[D_6]DMSO [M^{-1}]
G18	12
G19	10
G22	9
G23	22
G24	500[b]
G25	740[c]
G26	32
G27	5
G28	–
G29	7
G30	–
G31	–

[a] Error within ±10% from average of at least three titrations. Determinations were made directly using the signal from proton H_b. The symbol "–" denotes that binding was not observed. [b] Determinations were made by subtraction of H_e from free H_b. [c] Determinations were made by subtraction of H_e from (bound) H_{b*}.

binding was not observed until the relatively small bromocycloheptane (**G18**) was examined. In this case, and in the others reported here, the shift in the NMR signal of H_b demonstrated the expected "halogen down" binding. Models indicate that **G18** cannot fit under the methyl groups of **5**. Instead, to form the C–H···Br–R hydrogen bonds, the guest must adopt a conformation that places the bromine substituent in an equatorial position, while the seven-membered ring must slot between the methyl groups protruding into the cavity (Figure 4a). In this "vertical" orientation, the rotation of the guest

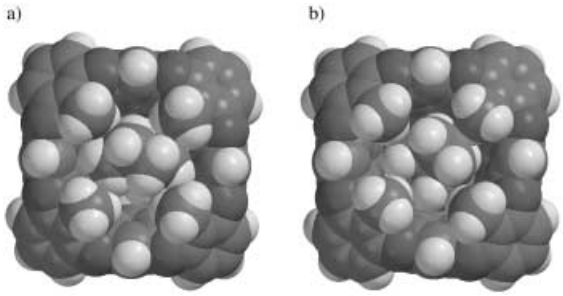

Figure 4. a) Space-filling model (generated from MMFF molecular mechanics (Spartan)) of bromocycloheptane (**G18**) binding to host **5**; b) Space-filling model of bromocyclopentane (**G24**) binding to host **5**.

around the C_4 axis of the host is inhibited by the inward pointing methyl groups. As a result binding is weak. Although bromocyclohexane (**G22**) appears to suffer the same fate, the binding of **G24** appears to be quite different. In the first instance, the association constant for bromocyclopentane (**G24**) is over twenty times that of **G22**, while the corresponding iodo derivative **G25** was found to bind even more strongly (3.9 kcal mol^{-1}). Furthermore, for **G24** and **G25**, binding is slow on the NMR timescale, whereas in the case of the cycloheptyl and cyclohexyl guests it is fast. This switch suggests a different mode of binding. Indeed, models indicate that **G24** and **G25** are small enough to bind underneath the rim methyl groups and still bind halogen down (Figure 4b), a mode of (horizontal) binding which would be promoted by the fact that halogen substituents in cyclopentyl systems show a preference for an axial orientation.[28] In this orientation, most of the protons experience a similar ("equatorial") environment. The exceptions, the H^3 and H^4 atoms on the opposite face to that occupied by the halogen atom, are located in the center of the cavity and facing the open portal. Hence, guest binding would be expected to lead to approximately two types of proton. EXSY NMR spectroscopy confirms this. Although it was not possible to assign all the signals of the guest, it was possible to determine that the signal from the methine proton shifted $\delta = -2.85$ ppm and those of six protons shifted between $\delta = -2.20$ and -2.32 ppm, while the signal from two hydrogens underwent only a shift of $\delta = -1.48$ ppm.[29]

Surprisingly the binding of cyclobutane derivative **G26** is both weak and fast on the NMR timescale. Likewise, no binding was observed with the aromatic guests **G30** and **G31**. Hence, host **5** is an extremely selective host for halocyclopentanes. With bromocycloalkanes, a methylene group either

  0947-6539/03/0901-0135 $ 20.00+.50/0

way of the cyclopentyl system makes binding less favorable by either 2.3 or 1.6 kcal mol^{-1}.

Van't Hoff analysis of selected host–guest associations: Tables 4 and 5 present a breakdown of the free energy of complexation of six adamantyl guests and iodocyclopentane binding to **3** and **4**. All of the host–guest interactions monitored displayed a negative entropic change. The approximate nanometer scale dimensions of these hosts suggest that small solvents could easily solvate the cavity in multiple numbers. Hence, our initial expectation was for the associations to be at least in part entropy driven. This is not the case at all. All complexations are not entropically favorable; this effect is least in chloroform and greatest in DMSO. Figure 5 graphs these changes for the typical guest **G9** binding to **4**, and emphasizes that enthalpy–entropy compensation as function of the solvent is observed.[30] The overall negative entropy values also suggest that the observed trend of stronger binding in DMSO is not a classic solvophobic effect.[31]

A closer examination of either set of results is illuminating. As expected, because it can freely tumble in the molecular cavity, the least entropically unfavorable guest is **G1**. The entropy becomes less favorable when the freedom of the guest is reduced to it spinning on one axis, in one particular orientation (**G9** to **G11**). Furthermore this effect increases as the halogen atom increases in size. Assuming that the entropic component of solvating each haloadamantane is a constant, these $\Delta\Delta S$ values in the series **G9**–**G11** reflect a progressive constraining of the C_3 rotation axis of the guest to the C_4 axis of the host as the halogen atom increases in size. Overall, these results reveal another level of enthalpy–entropy

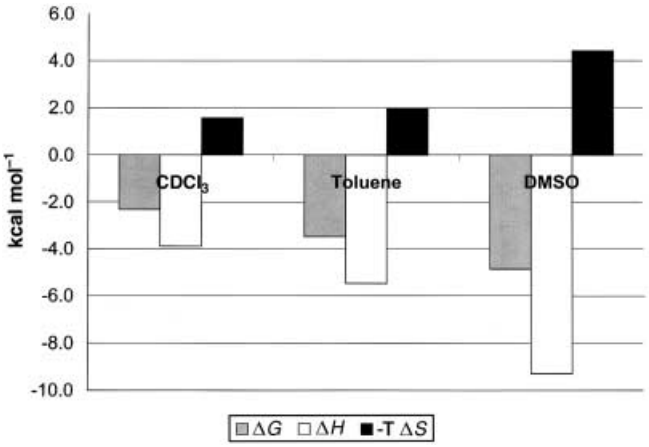

Figure 5. Enthalpy–entropy trends as a function of solvent for **G9** binding to basket **4**.

compensation, this time as a function of the functional group. Figure 6 graphs the trends for adamantanes binding to **4** in toluene.

A comparison of the two sets of data allows a more accurate picture of the strength of C–H···I–R hydrogen bonds. The complexation of adamantane (**G1**) to **3** (**4**) results in the release of 2.7 (3.2) kcal mol^{-1} enthalpy in "neutral" toluene. In contrast, when **G11** complexes there is an enthalpic stabilization of 9.4 (9.8) kcal mol^{-1}. One quarter of this difference corresponds to approximately 1.7 (1.6) kcal mol^{-1} per C–H···I–R interaction. Thus taking into account the probability that there will be some synergism, it seems reasonable to conclude that each hydrogen bond is capable of contributing at least 1 kcal mol^{-1} of stability.

Table 4. ^{1}H NMR derived thermodynamic parameters for the binding of selected adamantanes to host **3** at 298 K.[a]

Guest	$CDCl_3$ [kcal mol^{-1}]			[D_8]Toluene [kcal mol^{-1}]			[D_6]DMSO [kcal mol^{-1}]		
	ΔG	ΔH	$T\Delta S$	ΔG	ΔH	$T\Delta S$	ΔG	ΔH	$T\Delta S$
G1	–	–	–	–1.6	–2.7	–1.0	–4.0	–8.7	–4.7
G8	–	–	–	–	–	–	–3.7	–7.9	–4.2
G9	–2.3	–3.9	–1.6	–3.5	–5.5	–2.0	–4.9	–9.3	–4.4
G10	–3.3	–5.0	–1.7	–4.4	–7.9	–3.6	–	–	–
G11	–3.8	–7.3	–3.5	–5.1	–9.4	–4.4	–	–	–
G12	–2.6	–4.3	–1.7	–3.6	–5.7	–2.1	–5.5	–12.0	–6.5
G25	–	–	–	–	–	–	–3.2	–6.8	–3.6

[a] Errors are within ±15% for an average of at least two titrations. For each guest, the thermodynamic values were determined using the same NMR signals as those used for the determination of the association constants (see Table 1). The symbol "–" denotes that binding was too weak (or too strong) to determine the respective thermodynamic parameters.

Table 5. ^{1}H NMR derived thermodynamic parameters for the binding of selected adamantanes to host **4** at 298 K.[a]

Guest	$CDCl_3$ [kcal mol^{-1}]			[D_8]Toluene [kcal mol^{-1}]			[D_6]DMSO [kcal mol^{-1}]		
	ΔG	ΔH	$T\Delta S$	ΔG	ΔH	$T\Delta S$	ΔG	ΔH	$T\Delta S$
G1	–	–	–	–1.6	–3.2	–1.6	–4.2	–10.1	–6.0
G8	–	–	–	–	–	–	–3.8	–8.9	–5.1
G9	–2.5	–3.7	–1.2	–3.6	–6.3	–2.8	–5.1	–13.0	–7.9
G10	–3.4	–5.8	–2.4	–4.6	–8.2	–3.6	–	–	–
G11	–3.9	–7.0	–3.1	–5.2	–9.8	–4.6	–	–	–
G12	–2.5	–5.8	–3.3	–3.5	–7.8	–4.2	–5.6	–13.1	–7.5
G25	–	–	–	–	–	–	–3.3	–10.4	–7.0

[a] Errors are within ±15% for an average of at least two titrations. For each guest the thermodynamic values were determined using the same NMR signals as those used for the determination of the association constants (see Table 2). The symbol "–" denotes that binding was too weak (or too strong) to determine the respective thermodynamic parameters.

0947-6539/03/0901-0136 $ 20.00+.50/0 *Chem. Eur. J.* **2003**, *9*, No. 1

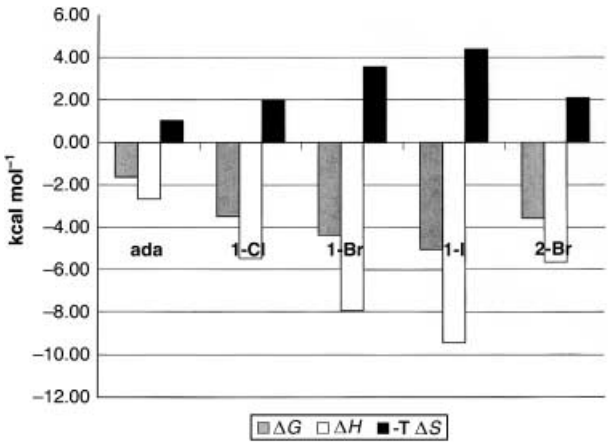

Figure 6. Enthalpy–entropy trends as a function of halogen atom for a number of substituted adamantanes binding to basket **4** in [D_8]toluene.

We also examined the binding of guests **G24**, **G25**, and **G18** to host **5** to look for further evidence suggesting a different mode of binding of the cycloheptane and cyclopentane derivatives. The thermodynamic parameters presented in Table 6 demonstrate that binding is again entropically unfavorable. For the cycloheptyl system, the entropic penalty is similar to those observed for the binding of guests to baskets **3** and **4**. However, the entropic cost for binding the cyclopentyl guests is twice that recorded for the cycloheptyl guest. The enthalpy changes with the complexation of cyclopentyl systems are also extremely high. For example, **G25** binds to *open* host **5** liberating 19 kcal mol^{-1}! The binding enthalpy of **G18** is half that value and more in line with the other systems. Assuming similar enthalpies and entropies of solvation for **G18** and **G24**, these differences strongly support the hypothesis that guests **G24** and **G25** do not bind in the same manner as **G18** (and presumably **G22** or **G23**). Rather cyclopentyl guests are just the perfect size to slip under the methyl groups at the rim of **5** and form some intimate contacts with both the crown of benzal hydrogens and the cavity wall (Figure 4b).

Table 6. ^{1}H NMR derived thermodynamic parameters for guest complexation to basket **5** at 298 K.[a]

Guest	[D_6]DMSO [kcal mol^{-1}]		
	ΔG	ΔH	$T\Delta S$
G18	−1.4	−8.5	−7.2
G24	−3.6	−17.6	−14.0
G25	−3.9	−18.6	−14.7

[a] Errors are within ±15% for an average of at least two titrations. For each guest the thermodynamic values were determined using the same NMR signals as those used for the determination of the association constants (see Table 3).

Conclusion

We have detailed the synthesis and binding properties of a new family of nanoscale molecular hosts. Their highly preorganized design, combined with a fully open cavity, allows them to bind a wide variety of guest molecules. Both the type of guests selected by each host and guest orientation within the molecular cavities are controlled by a number of factors including the shape of the cavity, the functionality on the guest, and the solvent used for complexation. Furthermore, the rigidity of these hosts results in radical differences in guest binding and orientation, even with closely related guests. However, the most important influence on guest selectivity and orientation is the functionality at the base of the cavity of each host. This crown of benzal hydrogens results in the preferential binding of halogenated derivatives by the formation of either bi-, tri-, or tetrafurcated acceptor type hydrogen bonds, depending on the type of halogen atom involved. Thus these hosts confirm the attractive nature of C–H···X–R hydrogen bonds and indicate the upper limit for these types of interactions to be 1.5 kcal mol^{-1}.

Experimental Section

General: All reagents and guests were purchased from Aldrich Chemical Company. Solvents were purchased from EM Science. Deuterated solvents were purchased from Cambridge Isotopes. Dimethylformamide (DMF) and dimethylacetamide (DMA) were stored over molecular sieves and degassed prior to use. Other reagents and guests were used as received. All reactions were run under a nitrogen atmosphere. Flash chromatography (silica gel 60 Å, 200–400 mesh; Natland International) was used for product purification.

^{1}H NMR spectra were recorded on a Varian Unity Inova instrument (500 MHz, 25 °C). The COSY spectra were run at 298 K using a homonuclear correlation pulse sequence (COSY macro supplied by Varian). A phase-sensitive NOE 2D correlation pulse sequence (NOESY macro supplied by Varian) was used to acquire 2D NOESY and 2D EXSY spectra. A mixing time of 0.5 s and a relaxation delay of 10 s were used. The number of $t1$ increments was 256 or 512, and 8 or 16 scans were accumulated at 298 K. Before Fourier transformation, a Gaussian apodization constant was applied on both dimensions. MS analysis was performed with a PerSeptive Biosystems Voyager Elite MALDI-TOF instrument. Elemental analysis was performed by Atlantic Microlab Inc. Melting points are uncorrected.

Multigram scale synthesis of 3,5-dibromobenzaldehyde:[11b] The compound 1,3,5-tribromobenzene (30 g, 95 mmol) and anhydrous diethyl ether (500 mL) were added to a dried flask. After stirring, the solution was cooled down to −78 °C, and *n*BuLi (45.4 mL, 95 mmol, 2.1 M solution in hexane) was added dropwise. After this addition, degassed anhydrous DMF (14.8 mL, 190 mmol) diluted in anhydrous diethyl ether (20 mL) was added dropwise, and the reaction stirred 1 h at −78 °C. The solution was then allowed to reach 0 °C and quenched with HCl (10%) until the solution was acidic. The mixture was partitioned between $CHCl_3$ and water, and the organic layer isolated. The aqueous layer was washed once with $CHCl_3$, and the organic layers were combined and dried with anhydrous $MgSO_4$. The solution was then concentrated under reduced pressure and run through a silica plug using a $CHCl_3$ mobile phase. Removal of the solvent under reduced pressure gave a colorless solid that was dried under reduced pressure for 1 h before the next step. The essentially pure 3,5-dibromobenzaldehyde was obtained in 94%.

Multigram scale synthesis of 3,5-dibromobenzal bromide:[11b] The 3,5-dibromobenzaldehyde (24 g, 90 mmol) was dissolved in dichloromethane (300 mL). BBr_3 (56 mL, 1.8 M) in dichloromethane (99 mmol) was added to this stirring solution. The reaction was stirred at RT for 24 h. The solution was then run though a silica column using hexane as the mobile phase (**CAUTION**, HBr fumes), and the solvent removed under reduced pressure. The reaction mixture was crystallized from hexane to give an 80% yield of the benzal bromide as large colorless crystals.

Multigram scale synthesis of DCC 2:[11b] The compound 3,5-dibromobenzal bromide (18 g, 44 mmol), degassed DMA (200 mL), and 1,8-diazabicyclo[5.4.0]undec-7-ene (DBU) (7.27 mL, 388 mmol) were added to a dried flask. With stirring, octol (5 g, 5.53 mmol) dissolved in DMA (50 mL) was

added by syringe pump over 64 h. The solution was then heated to 60 °C for four days. After this time the DMA was removed under reduced pressure, the mixture was partitioned between $CHCl_3$ and water, and the organic layer collected. The aqueous layer was washed twice with $CHCl_3$, and the organic layers were combined and dried with anhydrous $MgSO_4$. The solvent was reduced down to about 100 mL under reduced pressure. Silica gel (ca. 50 mL) was then added to the solution, and the solvent removed under reduced pressure. The dry silica was loaded on a 100% hexane silica column, and the excess 3,5 diBr-benzal bromide eluted with 100% hexane. The product was then eluted with 50% $CHCl_3$/hexane, and the solvent subsequently removed under reduced pressure. The crude product was then recrystallized from $CHCl_3$/hexane to give a 64% yield of the cavitand as a white solid.

Large-scale synthesis of basket 3:[7a] DCC **2** (1 g, 0.53 mmol), K_2CO_3 (877 mg, 6.3 mmol), resorcinol (350 mg, 3.18 mmol), and pyridine (65 mL) were added to a dried flask. Nitrogen was then bubbled through the solution for five minutes, before CuO (505 mg, 6.3 mmol) was carefully added. The flask was then fitted with a water condenser, and the stirring solution heated to reflux (sand bath) for seven days. After this time the solvent was removed under reduced pressure, and the resulting solid suspended in chloroform and flushed through a silica plug with $CHCl_3$ (100%). The solvent of the resulting solution was removed under reduced pressure, and the crude product further purified by column chromatography (mobile phase 50% $CHCl_3$/hexane). The product was isolated as a colorless solid in 78% yield (88% on the 250 mg scale).

Synthesis of basket 4: DCC **2** (100 mg, 5.30×10^{-5} mol) was added to an oven-dried round bottom flask containing pyridine (24 mL). K_2CO_3 (146.4 mg, 1.06 mmol) and 5-methyl resorcinol (65.8 mg, 0.53 mmol) were added to this stirring solution. Nitrogen was bubbled through the mixture for five minutes, before CuO (84.3 mg, 1.06 mmol) was added, and the solution was heated to a vigorous reflux (sand bath) and stirred for seven days. After cooling the solvent was removed under reduced pressure to give a crude solid mixture that was suspended in $CHCl_3$ and loaded onto a short silica plug. Flushing with $CHCl_3$ and removal of the solvent of the resulting colorless solution gave the crude product. Chromatography (1:1 $CHCl_3$/hexane) and then recrystallization with $CHCl_3$/hexane gave the pure product **4** as a colorless solid in 88% yield.

m.p. > 250 °C; ^{1}H NMR (500 MHz, $CDCl_3$): $\delta = 2.433$ (s, 12H), 2.55 (m, 16H), 4.56 (s, 4H), 4.84 (t, $J = 8$ Hz, 4H), 6.05 (s, 4H), 6.39 (t, $J = 2$ Hz, 4H), 6.52 (d, $J = 2$ Hz, 8H), 6.93 (t, $J = 2$ Hz, 4H), 7.00 (d, $J = 2$ Hz, 8H), 7.10 (m, 8H) 7.19 (m, 16H); MS: m/z: $[M+Ag^+]^+$ calcd 1845; found: 1845.97; elemental analysis calcd (%) for $C_{116}H_{88}O_{16}$: C 80.17, H 5.10; found: C 80.05, H 5.17.

Synthesis of basket 5: DCC **2** (100 mg, 5.30×10^{-5} mol) was added to an oven-dried round bottom flask containing pyridine (24 mL). K_2CO_3 (146.4 mg, 1.06 mmol) and 2-methyl resorcinol (65.8 mg, 0.53 mmol) were added to this stirring solution. Nitrogen was bubbled through for five minutes before CuO (84.3 mg, 1.06 mmol) was added, and the solution was heated to a vigorous reflux (sand bath) and stirred for 14 days. After cooling the solvent was removed under reduced pressure to give a crude solid mixture that was suspended in $CHCl_3$ and loaded onto a short silica plug. Flushing with $CHCl_3$ and removal of the solvent of the resulting pale yellow solution gave the crude product. Chromatography (1:1 $CHCl_3$/hexane) and then recrystallization with $CHCl_3$/hexane gave the pure product **5** as a colorless solid in 80% yield.

m.p. > 250 °C; ^{1}H NMR (500 MHz, $CDCl_3$): $\delta = 1.64$ (s, 12H), 2.53 (m, 16H), 4.50 (s, 4H), 4.81 (t, $J = 8$ Hz, 4H), 5.93 (s, 4H), 6.48 (d, $J = 1$ Hz, 8H), 7.04 (s, 4H), 7.09 (m, 8H), 7.14 (s, 4H), 7.20 (m, 20H), 7.40 (t, $J = 8$ Hz, 4H); MS: m/z: $[M+Ag^+]^+$ calcd 1845; found: 1845.38; elemental analysis calcd (%) for $C_{116}H_{88}O_{16} \cdot CHCl_3$: C 75.66, H 4.93; found: C 75.66, H 5.13.

Acknowledgements

This work was supported by the National Science Foundation (CHE-0111133), the Donors of the Petroleum Research Fund, administered by the American Chemical Society, and the Cancer Association of Greater New Orleans (CAGNO). Z.R.L. thanks the Louisiana BoR for a fellowship. Special thanks also to Richard B. Cole and the New Orleans Center for Mass Spectrometry Research for carrying out mass analysis of hosts **3**–**5**.

[1] a) P. Molenveld, J. F. J. Engbersen, D. N. Reinhoudt, *Chem. Soc. Rev.* **2000**, *29*, 75–86; b) J. P. Collman, L. Fu, *Acc. Chem. Res.* **1999**, *32*, 455–463; c) H. Vahrenkamp, *Acc. Chem. Res.* **1999**, *32*, 589–596; d) E. Kimura, T. Koike, *Chem. Commun.* **1998**, 1495–1501; e) R. Breslow, S. D. Dong, *Chem. Rev.* **1998**, *98*, 1997–2011; f) J. T. Groves, *Nature* **1997**, *389*, 329–330; g) P. A. Brady, J. K. M. Sanders, *Chem. Soc. Rev.* **1997**, *26*, 327–336; h) A. J. Kirby, *Angew. Chem.* **1994**, *106*, 573–576; *Angew. Chem. Int. Ed. Engl.* **1994**, *33*, 551–553; i) A. J. Kirby, *Angew. Chem.* **1996**, *108*, 770–790; *Angew. Chem. Int. Ed. Engl.* **1996**, *35*, 707–724; j) R. Breslow, *Acc. Chem. Res.* **1995**, *28*, 146–153; k) J. Chin, *Acc. Chem. Res.* **1991**, *24*, 145–152; l) J. F. Stoddart, *From Enzyme Mimics to Molecular Self-Assembly Processes in Chirality in Drug Design and Synthesis* (Ed.: C. Brown), Academic Press, San Diego, **1990**, pp. 53–81; m) J. W. Canary, B. C. Gibb, *Prog. Inorg. Chem.* **1997**, *45*, 1–81; n) R. P. Sijbesma, R. J. M. Nolte, *Molecular Clips and Cages Derived from Glycoluril* in *Supramolecular Chemistry II—Host Design and Molecular Recognition* (Ed.: E. Weber), Spinger, Berlin, **1995**, pp. 25–56.

[2] a) A. J. Kennan, V. Haridas, K. Severin, D. H. Lee, M. R. Ghadiri, *J. Am. Chem. Soc.* **2001**, *123*, 1797–1803; b) A. Saghatelian, Y. Yokobayashi, K. Soltani, M. R. Ghadiri, *Nature* **2001**, *409*, 797–801; c) D. H. Lee, J. R. Granja, J. A. Martinez, K. Severin, M. R. Ghadiri, *Nature* **1996**, *382*, 525–528; for minimal peptides with enantioselective acyl transfer properties see: d) G. T. Copeland, S. J. Miller, *J. Am. Chem. Soc.* **2001**, *123*, 6496–6502.

[3] For the synthesis of foldamers that could potentially be utilized for catalysis see: a) S. H. Gellman, *Acc. Chem. Res.* **1998**, *31*, 173–180; b) J. J. Barchi, Jr., X. Huang, D. H. Appella, L. A. Christianson, S. R. Durell, S. H. Gellman, *J. Am. Chem. Soc.* **2000**, *122*, 2711–2718; c) D. H. Appella, J. J. Barchi, Jr., S. R. Durell, S. H. Gellman, *J. Am. Chem. Soc.* **1999**, *121*, 2309–2310; d) A. Tanatani, M. J. Mio, J. S. Moore, *J. Am. Chem. Soc.* **2001**, *123*, 1792–1793; e) S. Lahiri, J. L. Thompson, J. S. Moore, *J. Am. Chem. Soc.* **2000**, *122*, 11315–11319; f) Y. Hamuro, S. J. Geib, A. D. Hamilton, *J. Am. Chem. Soc.* **1997**, *119*, 10587–10593; g) D. Seebach, S. Abele, K. Gademann, B. Juan, *Angew. Chem.* **1999**, *111*, 1700–1703; *Angew. Chem. Int. Ed.* **1999**, *38*, 1595–1597; h) K. Kirshenbaum, A. E. Barron, R. A. Goldsmith, P. Armand, E. K. Bradley, K. T. V. Truong, K. A. Dill, F. E. Cohen, R. N. Zuckermann, *Proc. Natl. Acad. Sci. USA* **1998**, *95*, 4303–4308; i) P. Armand, K. Kirshenbaum, R. A. Goldsmith, S. Farr-Jones, A. E. Barron, K. T. V. Truong, K. A. Dill, D. F. Mierke, F. E. Cohen, R. N. Zuckermann, E. K. Bradley, *Proc. Natl. Acad. Sci. USA* **1998**, *95*, 4309–4314; j) M. Habihara, N. J. Anthony, T. J. Stout, J. Clardy, S. L. Schreiber, *J. Am. Chem. Soc.* **1992**, *114*, 6568–6570; k) R. S. Lokey, B. L. Iverson, *Nature* **1995**, *375*, 303–305; l) D. M. Bassani, J.-M. Lehn, G. Baum, D. Fenske, *Angew. Chem.* **1997**, *109*, 1931–1933; *Angew. Chem. Int. Ed. Engl.* **1997**, *36*, 1845–1847.

[4] a) C. D. Gutsche, *Calixarenes Revisited*, Royal Society of Chemistry, London, **2000**; b) *Calixarenes in Action* (Eds.: L. Mandolini, R. Ungaro), Imperial College Press, London, **2000**.

[5] a) A. G. S. Högberg, *J. Org. Chem.* **1980**, *45*, 4498–4500; b) D. J. Cram, J. M. Cram, *Container Molecules and Their Guests*, Royal Society of Chemistry, Cambridge, **1994**.

[6] A. Collet in *Comprehensive Supramolecular Chemistry*, *Vol 2*, (Eds.: J.-M. Lehn, J. L. Atwood, J. E. D. Davies, D. D. MacNicol, F. Vögtle), Elsevier, London, **1996**, pp. 325–366.

[7] a) C. L. D. Gibb, E. D. Stevens, B. C. Gibb, *J. Am. Chem. Soc.* **2001**, *123*, 5849–5850; b) C. L. D. Gibb, X. Li, B. C. Gibb, *Proc. Natl. Acad. Sci. USA* **2002**, *99*, 4857–4862; c) C. L. D. Gibb, H. Xi, P. A. Politzer, M. Concha, B. C. Gibb, *Tetrahedron* **2002**, *58*, 673–681; d) N. Chopra, J. C. Sherman, *Angew. Chem.* **1999**, *111*, 2109–2111; *Angew. Chem. Int. Ed.* **1999**, *38*, 1955–1957; e) A. Jasat, J. C. Sherman, *Chem. Rev.* **1999**, *99*, 932–967; f) J. Kim, I.-S. Jung, S.-Y. Kim, E. Lee, J.-K. Kang, S. Sakamoto, K. Yamaguchi, K. Kim, *J. Am. Chem. Soc.* **2000**, *122*, 540–541.

[8] a) A. R. Renslo, J. Rebek, Jr., *Angew. Chem.* **2000**, *112*, 3419–3421; *Angew. Chem. Int. Ed.* **2000**, *39*, 3281–3283; b) P. L. Wash, A. R. Renslo, J. Rebek, Jr., *Angew. Chem.* **2001**, *113*, 1261–1262; *Angew. Chem. Int. Ed.* **2001**, *40*, 1221–1222; c) D. M. Rudkevich, J. Rebek, Jr., *Eur. J. Org. Chem.* **1999**, 1991–2005; d) A. R. Renslo, F. C. Tucci, D. M. Rudkevich, J. Rebek, Jr., *J. Am. Chem. Soc.* **2000**, *122*, 4573–4582; e) U. Lücking, F. C. Tucci, D. M. Rudkevich, J. Rebek, Jr.,

  0947-6539/03/0901-0138 $ 20.00+.50/0

J. Am. Chem. Soc. **2000**, *122*, 8880–8889; f) T. Haino, D. M. Rudkevich, J. Rebek, Jr., *J. Am. Chem. Soc.* **1999**, *121*, 11253–11254; g) F. C. Tucci, A. R. Renslo, D. M. Rudkevich, J. Rebek, Jr., *Angew. Chem.* **2000**, *112*, 1118–1121; *Angew. Chem. Int. Ed.* **2000**, *39*, 1076–1079; h) F. C. Tucci, D. M. Rudkevich, J. Rebek, Jr., *J. Org. Chem.* **1999**, *64*, 4555–4559.

[9] a) Y. Tanaka, C. Khare, M. Yonezawa, Y. Aoyama, *Tetrahedron Lett.* **1990**, *31*, 6193–6196; b) H. Ross, U. Lüning, *Tetrahedron Lett.* **1997**, *38*, 4539–4542; c) S. Blanchard, L. LeClainche, M.-N. Rager, J.-P. Tuchagues, A. F. Dupart, Y. LeMest, O. Reinaud, *Angew. Chem.* **1998**, *110*, 2861–2864; *Angew. Chem. Int. Ed.* **1998**, *37*, 2732–2735; d) O. Sénèque, M.-N. Rager, M. Giorgi, O. Reinaud, *J. Am. Chem. Soc.* **2001**, *123*, 8442–8443; e) Y. Rondelez, G. Bertho, O. Reinaud, *Angew. Chem.* **2002**, *114*, 1086–1088; *Angew. Chem. Int. Ed.* **2002**, *41*, 1044–1046; f) For general examples see the recent special issue of Chemical Reviews dedicated to enzyme mimicry (*Chem. Rev.* **1996**, *96*, 2237–3042).

[10] S. D. Starnes, D. M. Rudkevich, J. Rebek, Jr., *J. Am. Chem. Soc.* **2001**, *123*, 4659–4669.

[11] a) H. Xi, C. L. D. Gibb, E. D. Stevens, B. C. Gibb, *Chem. Commun.* **1998**, 1743–1744; b) H. Xi, C. L. D. Gibb, B. C. Gibb, *J. Org. Chem.* **1999**, *64*, 9286–9288; c) J. O. Green, J.-H. Baird, B. C. Gibb, *Org. Lett.* **2000**, *2*, 3845–3848.

[12] We now perform the synthesis of 3,5-dibromobenzal bromide at the 30 g scale. The procedures developed for this scale-up, the multigram synthesis of DCC **2**, and the gram scale syntheses of **3** are modified somewhat from those originally devised (see reference [7a]) and so are included in the Experimental Section.

[13] See for example: a) F. Theil, *Angew. Chem.* **1999**, *111*, 2493–2495; *Angew. Chem. Int. Ed.* **1999**, *38*, 2345–2347; b) D. M. T. Chan, K. L. Monaco, R.-P. Wang, M. P. Winters, *Tetrahedron Lett.* **1998**, *39*, 2933–2936; c) D. A. Evans, J. L. Katz, T. R. West, *Tetrahedron Lett.* **1998**, *39*, 2937–2940; d) J.-F. Marcoux, S. Doye, S. L. Buchwald, *J. Am. Chem. Soc.* **1997**, *119*, 10539–10540.

[14] Calculations were carried out using PC Spartan Pro version 1.0.6 (Wavefunction Inc.). All calculations were performed on C_{4v} structures that were abbreviated by substituting methyl for phenethyl feet. The models were built from a common ancestor, the (3,5-substituted) octaphenol deep-cavity cavitand (structure **2** but substituting OH for Br).

[15] For each host the signal corresponding to H_b was noted to broaden significantly as the temperature approached $-90\,^{\circ}C$. As we discuss in the main text, the benzal protons H_b are those most influenced by guest binding. By examining this phenomenon as a function of concentration, we discounted the possibility that the guests in this case were the "feet" of another molecule. Hence, the broadening arose from the exchange of solvent into and out of the cavity slowing down to the NMR timescale. Supporting evidence for this hypothesis was garnered when the temperature of solutions of **3** in CD_2Cl_2 with either guests **G11** or **G22** (Scheme 3) was lowered to $-90\,^{\circ}C$. Under these conditions no broadening of the signal H_b occurred.

[16] Assuming that at least a $\delta = 0.05$ ppm difference for a theoretical splitting of a suitable signal occurs, a coalescence temperature (T_c) of $-90\,^{\circ}C$ would give a rate constant ($k_c = 2.22\,\Delta v$) of 55.5 s^{-1}. Thus using the Eyring equation ($\Delta G^{\ddagger} = 4.58\ T_c[10.32 + \log(T_c/k_c)]$) the free energy of activation (ΔGv) for the flipping process must be less than approximately 9 kcal mol^{-1}. See: H. Friebolin, *Basic One- and Two-Dimensional NMR Spectroscopy*, 3rd revised ed., Wiley-VCH, Weinheim, **1998**.

[17] J. C. Adrian, Jr., C. S. Wilcox, *J. Am. Chem. Soc.* **1992**, *114*, 1398–1403.

[18] For a closed system displaying host–guest diastereomeric complexes see: P. Timmerman, W. Verboom, F. C. J. M. van Veggel, J. P. M. van Duynhoven, D. N. Reinhoudt, *Angew. Chem.* **1994**, *106*, 2437–2440; *Angew. Chem. Int. Ed. Engl.* **1994**, *33*, 2345–2348.

[19] The association constants for guests **G1**, **G7**–**G12**, **G14**, **G18**, **G22**–**G25**, **G27**–**G28**, and **G30**–**G31** to host **3** in both chloroform and toluene have been previously reported. See references [7a] and [7b].

[20] The errors associated with the quoted ΔG values ($\delta\Delta G$) are given by: $\delta\Delta G = -RT/K \times \delta K$; where δK is the error in measuring K ($\pm 10\,\%$). Thus, the errors are ± 0.05921 kcal mol^{-1}.

[21] In toluene, sigmoidal binding curves (commonly a sign of cooperativity but not possible in these hosts) were recorded for these guests binding to basket **3** (see: K. A. Connors, *Binding Constants*, Wiley Interscience, New York, **1987**; C. S. Wilcox, J. C. Adrian, T. H. Webb, F. J. Zawacki, *J. Am. Chem. Soc.* **1992**, *114*, 10189–10197).

[22] L. W. Deady, M. Kendall, R. D. Topsom, R. A. Y. Jones, *J. Chem. Soc. Perkin Trans. 2* **1973**, 416–420.

[23] G. C. Pimentel, A. L. McClennan, *The Hydrogen Bond*, W. H. Freeman, San Francisco, **1960**.

[24] H. Umeyama, K. Morokuma, *J. Am. Chem. Soc.* **1977**, *99*, 1316–1332.

[25] G. A. Jeffrey, *An Introduction to Hydrogen Bonds*, Oxford University Press, New York, **1997**

[26] G. R. Desiraju, T. Steiner, *The Weak Hydrogen Bond*, Oxford University Press, Oxford, **1999**.

[27] a) T. Spaniel, H. Görls, J. Scholz, *Angew. Chem.* **1998**, *110*, 1962–1966; *Angew. Chem. Int. Ed.* **1998**, *37*, 1862–1865; b) R. Taylor, O. Kennard, *J. Am. Chem. Soc.* **1982**, *104*, 5063–5070; c) O. Navon, J. Bernstein, V. Khodorkovsky, *Angew. Chem.* **1997**, *109*, 640–642; *Angew. Chem. Int. Ed. Engl.* **1997**, *36*, 601–603.

[28] a) R. L. Hilderbrandt, Q. Shen, *J. Phys. Chem.* **1982**, *86*, 587–593; b) X. Zheng, C. W. Lee, D. L. Philips, *J. Chem. Phys.* **1999**, *111*, 11034–11043.

[29] In contrast, a vertical mode of binding for **G24** would result in two sets of signal shifts integrating for four protons each, because the H^2/H^4 methylene groups would be bound more deeply than the H^3/H^4 methylene groups.

[30] a) M. S. Westwell, M. S. Searle, J. Klein, D. H. Williams, *J. Phys. Chem.* **1996**, *100*, 16000–16001; b) C. T. Calderone, D. H. Williams, *J. Am. Chem. Soc.* **2001**, *123*, 6262–6267, and references therein; c) D. H. Williams, D. P. O'Brien, B. Bardsley, *J. Am. Chem. Soc.* **2001**, *123*, 737–738.

[31] A. Marmur, *J. Am. Chem. Soc.* **2000**, *122*, 2120–2121.

Received: June 5, 2002 [F4157]

  0947-6539/03/0901-0139 $ 20.00+.50/0